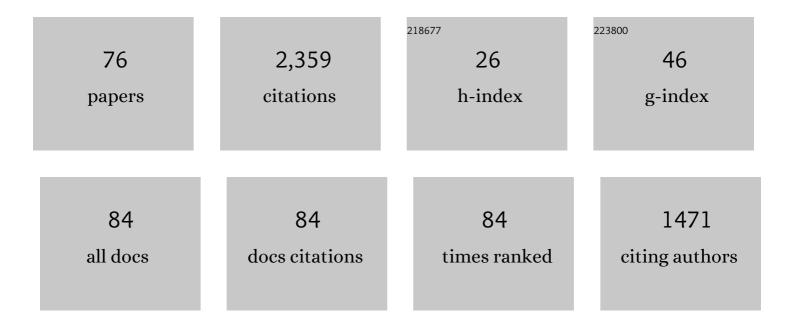
List of Publications by Year in descending order

Source: https://exaly.com/author-pdf/1079508/publications.pdf Version: 2024-02-01



IAN-REDNO HÃOVENED

| # | Article | IF | CITATIONS |
|----|--|-----|-----------|
| 1 | Multimodal Targeted Nanoparticle-Based Delivery System for Pancreatic Tumor Imaging in Cellular and Animal Models. Current Pharmaceutical Design, 2022, 28, 313-323. | 1.9 | 10 |
| 2 | Instrumentation for Hydrogenative Parahydrogen-Based Hyperpolarization Techniques. Analytical Chemistry, 2022, 94, 479-502. | 6.5 | 52 |
| 3 | Dynamic <i>in vivo</i> monitoring of fracture healing process in response to magnesium implant with multimodal imaging: pilot longitudinal study in a rat external fixation model. Biomaterials Science, 2022, 10, 1532-1543. | 5.4 | 14 |
| 4 | Influence of Spatial Resolution and Compressed SENSE Acceleration Factor on Flow Quantification with 4D Flow MRI at 3 Tesla. Tomography, 2022, 8, 457-478. | 1.8 | 4 |
| 5 | Frequencyâ€Selective Manipulations of Spins allow Effective and Robust Transfer of Spin Order from Parahydrogen to Heteronuclei in Weakly oupled Spin Systems. ChemPhysChem, 2022, 23, . | 2.1 | 10 |
| 6 | Quasi-continuous production of highly hyperpolarized carbon-13 contrast agents every 15 seconds within an MRI system. Communications Chemistry, 2022, 5, . | 4.5 | 15 |
| 7 | Symmetry Constraints on Spin Order Transfer in Parahydrogen-Induced Polarization (PHIP). Symmetry, 2022, 14, 530. | 2.2 | 6 |
| 8 | High-Resolution Single Tooth MRI With an Inductively Coupled Intraoral Coil—Can MRI Compete With CBCT?. Investigative Radiology, 2022, 57, 720-727. | 6.2 | 11 |
| 9 | Performance and reproducibility of 13C and 15N hyperpolarization using a cryogen-free DNP polarizer. Scientific Reports, 2022, 12, . | 3.3 | 15 |
| 10 | Catalytic Hydrogenation of Trivinyl Orthoacetate: Mechanisms Elucidated by Parahydrogen Induced Polarization. ChemPhysChem, 2021, 22, 370-377. | 2.1 | 4 |
| 11 | Selective excitation doubles the transfer of parahydrogen-induced polarization to heteronuclei. Physical Chemistry Chemical Physics, 2021, 23, 14146-14150. | 2.8 | 9 |
| 12 | High field <i>para</i> hydrogen induced polarization of succinate and phospholactate. Physical Chemistry Chemical Physics, 2021, 23, 2320-2330. | 2.8 | 8 |
| 13 | Open-source, partially 3D-printed, high-pressure (50-bar) liquid-nitrogen-cooled parahydrogen generator. Magnetic Resonance, 2021, 2, 49-62. | 1.9 | 22 |
| 14 | 3Dâ€printed, patientâ€specific intracranial aneurysm models: From clinical data to flow experiments with endovascular devices. Medical Physics, 2021, 48, 1469-1484. | 3.0 | 14 |
| 15 | <scp>Pseudoâ€Enhancement</scp> in Intracranial Aneurysms on <scp>Blackâ€Blood MRI</scp> : Effects of Flow Rate, Spatial Resolution, and Additional Flow Suppression. Journal of Magnetic Resonance Imaging, 2021, 54, 888-901. | 3.4 | 16 |
| 16 | Telmisartan prevents high-fat diet-induced neurovascular impairments and reduces anxiety-like behavior. Journal of Cerebral Blood Flow and Metabolism, 2021, 41, 2356-2369. | 4.3 | 13 |
| 17 | Thinâ€Film Patientâ€Specific Flow Diverter Stents for the Treatment of Intracranial Aneurysms. Advanced Materials Technologies, 2021, 6, 2100384. | 5.8 | 2 |
| 18 | A realistic way to investigate the design, and mechanical properties of flow diverter stents. Expert Review of Medical Devices, 2021, 18, 569-579. | 2.8 | 3 |

| # | Article | IF | CITATIONS |
|----|--|------|-----------|
| 19 | Parahydrogen-Induced Polarization Relayed via Proton Exchange. Journal of the American Chemical Society, 2021, 143, 13694-13700. | 13.7 | 18 |
| 20 | Parawasserstoffâ€induzierte Polarisation von Aminosären. Angewandte Chemie, 2021, 133, 23688. | 2.0 | 2 |
| 21 | Parahydrogenâ€Induced Polarization of Amino Acids. Angewandte Chemie - International Edition, 2021, 60, 23496-23507. | 13.8 | 34 |
| 22 | Coherent Evolution of Signal Amplification by Reversible Exchange in Two Alternating Fields (alt‧ABRE). ChemPhysChem, 2021, 22, 2381-2386. | 2.1 | 14 |
| 23 | Luminal enhancement in intracranial aneurysms: fact or feature?—A quantitative multimodal flow analysis. International Journal of Computer Assisted Radiology and Surgery, 2021, 16, 1999-2008. | 2.8 | 2 |
| 24 | Selective excitation of hydrogen doubles the yield and improves the robustness of parahydrogen-induced polarization of low-γ nuclei. Physical Chemistry Chemical Physics, 2021, 23, 26645-26652. | 2.8 | 15 |
| 25 | Continuous Radio Amplification by Stimulated Emission of Radiation using Parahydrogen Induced Polarization (PHIPâ€RASER) at 14 Tesla. ChemPhysChem, 2020, 21, 667-672. | 2.1 | 25 |
| 26 | Pulse-Programmable Magnetic Field Sweeping of Parahydrogen-Induced Polarization by Side Arm Hydrogenation. Analytical Chemistry, 2020, 92, 1340-1345. | 6.5 | 28 |
| 27 | Intratumoral Distribution of Lactate and the Monocarboxylate Transporters 1 and 4 in Human Glioblastoma Multiforme and Their Relationships to Tumor Progression-Associated Markers. International Journal of Molecular Sciences, 2020, 21, 6254. | 4.1 | 13 |
| 28 | Dynamic 2D and 3D mapping of hyperpolarized pyruvate to lactate conversion in vivo with efficient multiâ€echo balanced steadyâ€state free precession at 3 T. NMR in Biomedicine, 2020, 33, e4291. | 2.8 | 16 |
| 29 | Coherent polarization transfer in chemically exchanging systems. Physical Chemistry Chemical Physics, 2020, 22, 8963-8972. | 2.8 | 4 |
| 30 | Ni(II)porphyrins as pH dependent light-driven coordination-induced spin-state switches (LD-CISSS) in aqueous solution. Journal of Porphyrins and Phthalocyanines, 2020, 24, 480-488. | 0.8 | 7 |
| 31 | Virtual implant planning and fully guided implant surgery using magnetic resonance imaging—Proof of principle. Clinical Oral Implants Research, 2020, 31, 575-583. | 4.5 | 29 |
| 32 | In vitro singlet state and zero-quantum encoded magnetic resonance spectroscopy: Illustration with N-acetyl-aspartate. PLoS ONE, 2020, 15, e0239982. | 2.5 | 6 |
| 33 | Simulating Nonâ€inear Chemical and Physical (CAP) Dynamics of Signal Amplification By Reversible Exchange (SABRE). Chemistry - A European Journal, 2019, 25, 7580-7580. | 3.3 | 2 |
| 34 | SAMBADENA Hyperpolarization of ¹³ Câ€Succinate in an MRI: Singletâ€Triplet Mixing Causes Polarization Loss. ChemistryOpen, 2019, 8, 728-736. | 1.9 | 25 |
| 35 | Zero-field nuclear magnetic resonance of chemically exchanging systems. Nature Communications, 2019, 10, 3002. | 12.8 | 36 |
| 36 | Multiple Quantum Coherences Hyperpolarized at Ultra‣ow Fields. ChemPhysChem, 2019, 20, 2823-2829. | 2.1 | 14 |

1

| # | Article | IF | CITATIONS |
|----|--|------|-----------|
| 37 | Lifetime of Para hydrogen in Aqueous Solutions and Human Blood. ChemPhysChem, 2019, 20, 2408-2412. | 2.1 | 8 |
| 38 | Simulating Nonâ€linear Chemical and Physical (CAP) Dynamics of Signal Amplification By Reversible Exchange (SABRE). Chemistry - A European Journal, 2019, 25, 7659-7668. | 3.3 | 25 |
| 39 | Non-contrast-enhanced magnetic resonance imaging for visualization and quantification of endovascular aortic prosthesis, their endoleaks and aneurysm sacs at 1.5â€T. Magnetic Resonance Imaging, 2019, 60, 164-172. | 1.8 | 16 |
| 40 | ¹⁵ N MRI of SLICâ€SABRE Hyperpolarized ¹⁵ N‣abelled Pyridine and Nicotinamide. Chemistry - A European Journal, 2019, 25, 8465-8470. | 3.3 | 33 |
| 41 | Dendronised Ni(<scp>ii</scp>) porphyrins as photoswitchable contrast agents for MRI. Physical Chemistry Chemical Physics, 2019, 21, 24296-24299. | 2.8 | 12 |
| 42 | Optimization of 3D phase contrast venography for the assessment of the cranio-cervical venous system at 1.5ÅT. Neuroradiology, 2019, 61, 293-304. | 2.2 | 8 |
| 43 | Parahydrogenâ€Based Hyperpolarization for Biomedicine. Angewandte Chemie - International Edition, 2018, 57, 11140-11162. | 13.8 | 251 |
| 44 | Magnetic resonance imaging—a diagnostic tool for postoperative evaluation of dental implants: a case report. Oral Surgery, Oral Medicine, Oral Pathology and Oral Radiology, 2018, 125, e103-e107. | 0.4 | 21 |
| 45 | A mild case of molybdenum cofactor deficiency defines an alternative route of MOCS1 protein maturation. Journal of Inherited Metabolic Disease, 2018, 41, 187-196. | 3.6 | 16 |
| 46 | In vivo 13C-MRI using SAMBADENA. PLoS ONE, 2018, 13, e0200141. | 2.5 | 35 |
| 47 | Simultaneous characterization of tumor cellularity and the Warburg effect with PET, MRI and hyperpolarized ¹³ C-MRSI. Theranostics, 2018, 8, 4765-4780. | 10.0 | 35 |
| 48 | Only Para-Hydrogen Spectroscopy (OPSY) Revisited: In-Phase Spectra for Chemical Analysis and Imaging. Journal of Physical Chemistry A, 2018, 122, 8948-8956. | 2.5 | 13 |
| 49 | OnlyParahydrogen SpectrosopY (OPSY) pulse sequences – One does not fit all. Journal of Magnetic Resonance, 2018, 297, 86-95. | 2.1 | 8 |
| 50 | Chemical Exchange Reaction Effect on Polarization Transfer Efficiency in SLIC-SABRE. Journal of Physical Chemistry A, 2018, 122, 9107-9114. | 2.5 | 33 |
| 51 | Response to the letter to the editor regarding "Magnetic resonance imaging (MRI)—a diagnostic tool for postoperative evaluation of dental implants: a case report― Oral Surgery, Oral Medicine, Oral Pathology and Oral Radiology, 2018, 126, 444-445. | 0.4 | 0 |
| 52 | Parawasserstoffâ€basierte Hyperpolarisierung für die Biomedizin. Angewandte Chemie, 2018, 130, 11310-11333. | 2.0 | 54 |
| 53 | Metabolic and Molecular Imaging with Hyperpolarised Tracers. Molecular Imaging and Biology, 2018, 20, 902-918. | 2.6 | 18 |
| | | | |

54 NMR Spectroscopy Techniques: Hyperpolarization for Sensitivity Enhancement. , 2018, , 168-168.

| # | Article | IF | CITATIONS |
|----|---|------|-----------|
| 55 | MRI. , 2017, , 227-324. | | 2 |
| 56 | Dental MRI using wireless intraoral coils. Scientific Reports, 2016, 6, 23301. | 3.3 | 78 |
| 57 | Molecular Imaging of Activated Platelets Allows the Detection of Pulmonary Embolism with Magnetic Resonance Imaging. Scientific Reports, 2016, 6, 25044. | 3.3 | 18 |
| 58 | Magnetic resonance imaging of intraoral hard and soft tissues using an intraoral coil and FLASH sequences. European Radiology, 2016, 26, 4616-4623. | 4.5 | 44 |
| 59 | Molecular MRI in the Earth's Magnetic Field Using Continuous Hyperpolarization of a Biomolecule in Water. Journal of Physical Chemistry B, 2016, 120, 5670-5677. | 2.6 | 37 |
| 60 | Quantitative description of the SABRE process: rigorous consideration of spin dynamics and chemical exchange. RSC Advances, 2016, 6, 24470-24477. | 3.6 | 55 |
| 61 | Evaluation of BP-ONJ in osteopenic and healthy sheep: comparing ZTE-MRI with µCT. Dentomaxillofacial Radiology, 2016, 45, 20150250. | 2.7 | 4 |
| 62 | Modular Coils with Low Hydrogen Content Especially for MRI of Dry Solids. PLoS ONE, 2015, 10, e0139763. | 2.5 | 9 |
| 63 | Toward Biocompatible Nuclear Hyperpolarization Using Signal Amplification by Reversible Exchange: Quantitative <i>in Situ</i> Spectroscopy and High-Field Imaging. Analytical Chemistry, 2014, 86, 1767-1774. | 6.5 | 105 |
| 64 | Continuous Reâ€hyperpolarization of Nuclear Spins Using Parahydrogen: Theory and Experiment. ChemPhysChem, 2014, 15, 2451-2457. | 2.1 | 41 |
| 65 | Wholeâ€body MRIâ€based fat quantification: A comparison to air displacement plethysmography. Journal of Magnetic Resonance Imaging, 2014, 40, 1437-1444. | 3.4 | 40 |
| 66 | A continuousâ€flow, highâ€throughput, highâ€pressure parahydrogen converter for hyperpolarization in a clinical setting. NMR in Biomedicine, 2013, 26, 124-131. | 2.8 | 83 |
| 67 | A hyperpolarized equilibrium for magnetic resonance. Nature Communications, 2013, 4, 2946. | 12.8 | 126 |
| 68 | A battery-driven, low-field NMR unit for thermally and hyperpolarized samples. Magnetic Resonance Materials in Physics, Biology, and Medicine, 2013, 26, 491-499. | 2.0 | 33 |
| 69 | On the spin order transfer from parahydrogen to another nucleus. Journal of Magnetic Resonance, 2012, 225, 25-35. | 2.1 | 68 |
| 70 | Dental MRI: Imaging of soft and solid components without ionizing radiation. Journal of Magnetic Resonance Imaging, 2012, 36, 841-846. | 3.4 | 75 |
| 71 | Fast volumetric spatial-spectral MR imaging of hyperpolarized 13C-labeled compounds using multiple echo 3D bSSFP. Magnetic Resonance Imaging, 2010, 28, 459-465. | 1.8 | 27 |
| 72 | Quality assurance of PASADENA hyperpolarization for 13C biomolecules. Magnetic Resonance Materials in Physics, Biology, and Medicine, 2009, 22, 123-134. | 2.0 | 79 |

| # | Article | IF | CITATIONS |
|----|---|------|-----------|
| 73 | PASADENA hyperpolarization of 13C biomolecules: equipment design and installation. Magnetic Resonance Materials in Physics, Biology, and Medicine, 2009, 22, 111-121. | 2.0 | 123 |
| 74 | PASADENA Hyperpolarization of Succinic Acid for MRI and NMR Spectroscopy. Journal of the American Chemical Society, 2008, 130, 4212-4213. | 13.7 | 170 |
| 75 | Whole-Brain <i>N</i> -Acetylaspartate MR Spectroscopic Quantification: Performance Comparison of Metabolite versus Lipid Nulling. American Journal of Neuroradiology, 2008, 29, 1441-1445. | 2.4 | 10 |
| 76 | MR Spectroscopy in Diagnosis and Neurological Decision-Making. Seminars in Neurology, 2008, 28, 407-422. | 1.4 | 27 |